Available online at www.sciencedirect.com
ScienceDirect
Catalysis Today 116 (2006) 478–484
CATALYSIS TODAY
www.elsevier.com/locate/cattod

# HDS and deep HDS activity of CoMoS-mesostructured clay catalysts

K.A. Carrado [a,*], J.H. Kim [b], C.S. Song [b], N. Castagnola [a], C.L. Marshall [c], M.M. Schwartz [c]

[a] *Chemistry Division, 9700 S. Cass Avenue, Argonne National Laboratory, Argonne, IL 60439, USA*
[b] *Clean Fuels & Catalysis Program, The Energy Institute and Department of Energy & Geo-Environmental Engineering, 206 Hosler Building, Pennsylvania State University, University Park, PA 16802, USA*
[c] *Chemical Engineering Division, 9700 S. Cass Avenue, Argonne National Laboratory, Argonne, IL 60439, USA*

Available online 1 August 2006

**Abstract**

The goal of this work is to identify more promising supports from synthetic clay materials to advance hydrotreating catalyst development. Silica sol can be used as the silicon-containing starting material when creating nanoporous layered silicate catalysts with a certain portion of unreacted sol particles incorporated into the final matrix. The resulting structure then has mesoporosity and a unique morphology. Hectorite-based clays have been prepared using different silica sols in order to ascertain the importance of sol characteristics on the final matrix. Several techniques have been applied to characterize the materials, including XRD, TGA, $N_2$ porosimetry, and TEM. For hydrodesulfurization (HDS), the conversion of dibenzothiophene (DBT) to biphenyl was examined at 400 °C using CoMoS-loaded mesostructured clay supports. No hydrogenation or hydrocracking was observed with any of the clay supports. The most active clay was derived from Ludox silica sol AS-30 with an activity of 65% DBT conversion and 100% selectivity to biphenyl (BP). For comparison, a reference commercial catalyst displayed 94% BP selectivity. For deep HDS, the conversion of 4,6-dimethyldibenzothiophene was tested at 325 and 350 °C. At 325 °C, conversions are 92% of commercial catalysts for a CoMoS-loaded mesostructured clay derived from Ludox AM-30 silica sol. A commercially available synthetic hectorite called laponite has very low activity, indicating that the unique morphology of the mesostructured clays is important. Hydrogenolysis vs. hydrogenation pathways are compared for the deep HDS reaction. HR-TEM of the most active deep HDS catalyst revealed a multilayered $MoS_2$ morphology.


*Keywords:* HDS activity; CoMoS; Clay catalysys

## 1. Introduction

In two recent reviews, Bej et al. [1a] and Song [1b] summarize the current status of efficient deep hydrodesulfurization (HDS) catalyst design. The reactivity of 4,6-dimethyldibenzothiophene (DMDBT) can be enhanced either by increasing the rate of direct desulfurization or by transformation to a more activated molecule through hydrogenation, isomerization, demethylation, and C–C bond scission. Towards the development of better catalysts using these concepts, different additives have been added to the traditional alumina support; in addition, other supports such as zeolites, zirconia, or titania, either by themselves or as mixtures with alumina, have been examined. It is then pointed out that non-alumina-based oxide-supported catalysts comprise a ''new horizon'' in HDS catalysis research. There are several publications regarding thiophene HDS over non-alumina-based catalysts [2]. However, since very few studies have been reported involving the HDS of DMDBT using such materials, the review predicts that there are ''immense opportunities'' for advances in this area. For example, Landau et al. [3] report that the activity of a silica-supported NiMo catalyst for the HDS of DMDBT is higher than that of both CoMo– and NiMo–$Al_2O_3$ catalysts. It is in this spirit that the present project was undertaken. The overall interest lies in identifying more promising supports, specifically from the synthetic clay materials, to advance hydrotreating catalyst development.

Also included in this category of strictly ''non-alumina-based'' (deep) HDS catalyst supports are zeolites and mesoporous materials. Because of their higher surface areas,

* Corresponding author. Tel.: +1 630 252 7968; fax: +1 630 252 9288.
*E-mail address:* kcarrado@anl.gov (K.A. Carrado).

0920-5861/$ – see front matter © 2006 Elsevier B.V. All rights reserved.
doi:10.1016/j.cattod.2006.06.033

acidic properties, and well-defined pore structures, these systems have attracted much interest as supports for CoMo- and NiMo-based HDS catalysts [4]. For example, Bataille et al. [5] studied the HDS of DMDBT over dealuminated HY-zeolite-supported Co and CoMo catalysts, and both catalysts exhibited higher rates compared to Mo– and CoMo–$Al_2O_3$ catalysts. Mesoporous materials such as MCM-41 possess the potential for higher diffusion rates for DMDBT. Although some research has been conducted using Mo- or CoMo-loaded MCM-41 for the HDS of DBT [6], only a few studies have been carried out for the HDS of DMDBT [4a,b]. Also falling into this category is the mesoporous titania studied by Dzwigaj et al. [2g]. It is stated by Bej et al. [1a] that further studies are required to understand and explore the full potential of these novel materials for deep HDS. In addition, the importance of new design approaches to ultra-clean diesel fuels by deep HDS has been pointed out recently [1b,7].

Because of their characteristic porous structure, surface reactivity, and ion exchange capacity, clays comprise another class of useful catalysts and catalyst supports [8]. They are essentially the two-dimensional, layered analogs of three-dimensional zeolites. Scattered reports exist in the literature concerning the HDS activity of clays, primarily pillared clays, with relatively few concentrating on CoMoS or NiMoS versions [9]. A study employing a synthetic high porosity saponite (a magnesium silicate clay) support with Pd–Rh promoted cobalt has been reported [10].

Over the years, our group has developed and patented a general technique for the hydrothermal synthesis of magnesium silicate hectorite clays in the presence of inorganic, organic, organometallic and polymeric intercalants [11]. This process involves the hydrothermal crystallization of a gel containing silica sol, magnesium hydroxide sol, lithium fluoride, and an alkylammonium cation or polymer if an organo-hectorite is desired. Because a certain portion of unreacted sol particles is incorporated into the final matrix, the resulting structure has mesoporosity and a unique morphology [12]. Previous reports concerning the feasibility of these materials as supports for HDS have been published [13]. Here we report on the preparation using different silica sols in order to examine the importance of sol particle size, pH, and surface chemistry on the final matrix. The test catalytic reactions are based on hydrodesulfurization reactivity, including deep HDS.

## 2. Experimental

### 2.1. Materials

The mesostructured clays were prepared according to published methods [11]. A 2 wt.% gel of silica sol, magnesium hydroxide sol, lithium fluoride, and optional organic is subject to aqueous reflux for 2 days. Reagents were purchased from Aldrich. The organic of choice for these crystallization studies is tetraethylammonium chloride (TEA). Precursor clay gels are of the composition:

$$0.32\mathrm{TEA}, 1.0\mathrm{LiF}, 5.3\mathrm{Mg(OH)_2}, 8\mathrm{SiO_2}, n\mathrm{H_2O}$$

to correlate with the ideal hectorite composition [14] of $Ex_{0.66}[Li_{0.66}Mg_{5.34}Si_8O_{20}(OH,F)_4]$, where Ex = exchangeable cation (Li, TEA). Note that Li(I) is also an isomorphous substitution for Mg(II) at about 1:9.6. Powder samples are isolated after centrifuging, washing, and drying. The silica sols include Ludox HS-30, SM-30, AM-30, AS-30, and TM-40. This represents a variety of sol particle sizes, pH values, and counter-ions as shown in Table 1. The sol particle sizes as provided by the supplier are compared to those measured using TEM in the final clay product; there are differences between these values as seen in Table 1. Both TEA- and lithium(I) (Li)-containing versions of the clays were made and denoted by the terms TEA-15hs or Li-24tm, for example. The numbers correspond to the size, in nm, of the silica sol as observed by TEM in the final product. Calcination was performed by heating the clay to 400 °C in a $N_2$ atmosphere and then to 500 °C in air prior to metal loading for HDS. Laponite RD was obtained from Southern Clay Products, Gonzales, TX.

### 2.2. Characterization

XRD patterns of powders were recorded on a Rigaku Miniflex+ with Cu Kα radiation, a 0.05° 2$\theta$ step size, and 0.5° 2$\theta$ scan rate. TEM images were acquired using a FEI TECNAI F30ST operating at 300 kV with a CCD camera. One drop of clay slurry in methanol (sonicated for 1 h) was placed onto 3 mm holey carbon Cu grids; excess solution was removed and the grid dried at 100 °C for 10 min. $N_2$ porosimetry was obtained on a Micromeritics ASAP2010 after degassing at 110 °C for at least 3 h and employing the multipoint BET and BJH methods.

Table 1
Synthetic clays based on silica sol source

| Clay support (template-silica sol size) | Ludox sol | Precursor silica sol pH[a] | Precursor silica sol diameter[a] (nm) | Average silica diameter in clay[b] (nm) |
|---|---|---|---|---|
| TEA-11sm | SM-30 | 10.2 | 7 | 11 |
| TEA-15hs | HS-30 | 9.8 | 12 | 15 |
| TEA-15am | AM-30 | 8.9 | 12 | 15 |
| TEA-15as | AS-30 | 9.2 | 22 | 15 |
| TEA-24tm | TM-40 | 9.0 | 22 | 24 |
| Li-24tm | TM-40 | 9.0 | 22 | 24 |

[a] As reported by the supplier.
[b] Determined via TEM analysis of the clay product.

### 2.3. HDS catalysis

For catalyst preparation, 4 g clay support was impregnated with $(NH_4)_6Mo_7O_{24}{\cdot}4H_2O$ (Aldrich) solution to give 6% Mo, dried at 110 °C for 1 h, and calcined at 400 °C for 4 h. The cooled catalyst was then impregnated with $Co(NO_3)_2{\cdot}6H_2O$ (Baker) solution to give 2% Co, dried at 110 °C for 1 h, calcined at 400 °C for 4 h. The catalysts were then pelletized in a Carver press, crushed and sieved retaining 10–20 mesh portion, heated under $N_2$ at 280 °C for 1 h and then sulfided with 8% $H_2S$ in $H_2$ at 350 °C for 2 h and re-sieved to 10–20 mesh. One gram sulfided and sieved catalyst was mixed with 2.0 g SiC (20 mesh; Electro Abrasives) and loaded into the trickle-bed reactor, a thick-walled 0.375 in. i.d. 316 SS tube that is mounted vertically in a three zone furnace. The catalyst is located in the center of the tube between plugs of quartz wool and on top of a deadman used to minimize the volume between the reactor and the liquid receiver. The liquid test feed consisted of 0.25 wt.% sulfur as dibenzothiophene (DBT) in hexadecane (1.4 wt.% DBT). The reaction was carried out at 400 °C under 286 psig $H_2$ (400 psig $H_2$ plus $N_2$; $N_2$ was added to provide control over and flexibility of space velocity) with WHSV = 15–18. After a sloped fore-cut of 3 or 4 h to reach steady-state, 2 or 3 one hour samples were collected, analyzed, and the results averaged. The reproducibility of the conversion measurements was ±4% of the reported values; mass balances were 100 ± 2%. The reaction products were diluted with mixed hexanes (0.3–0.7 g in 10.0 ml), separated using a DB5-MS column, and analyzed using an HP 5890A GC-MS. The reaction products are biphenyl and unconverted DBT.

### 2.4. Deep HDS catalysis

A two-step wet impregnation method was used to load the catalyst. First, 9 wt.% Mo is added in water from ammonium heptamolybdate tetrahydrate. After drying and calcination, 2.4 wt.% Co is added in water as cobalt(II) nitrate hexahydrate. The catalysts are dried at 110 °C overnight, calcined in air at 500 °C for 5 h, then pre-sulfided at 350 °C over a 4-h ramp and held for 2 h in 5% $H_2S$–$H_2$ using a flow apparatus. The catalysts were stored in decalin after presulfidation. HDS of 1.23 wt.% 4,6-dimethyldibenzothiophene (DMDBT) in decalin solvent was performed at 325 and 350 °C for 30 min under an initial hydrogen pressure of 300 psi (20.4 atm). Performance was compared to a Criterion 344 CoMoS–alumina catalyst (Cr344, 9.0 wt.% Mo, 2.35% Co) [15]. A microbatch reactor of 25 ml volume was employed using 4.0 g of feed and 0.10 g of catalyst. The reactor was placed in a preheated (325 or 350 °C) fluidized sand bath and agitated at 200 strokes/min. Following the reaction, the reactor was removed from the sand bath and immediately quenched in a cold-water bath. Products were analyzed by GC–MS (Shimadzu GC17A/QP-500) for identification and also by gas chromatography (GC SRI 8610C) equipped with an FID detector for quantitative analysis.

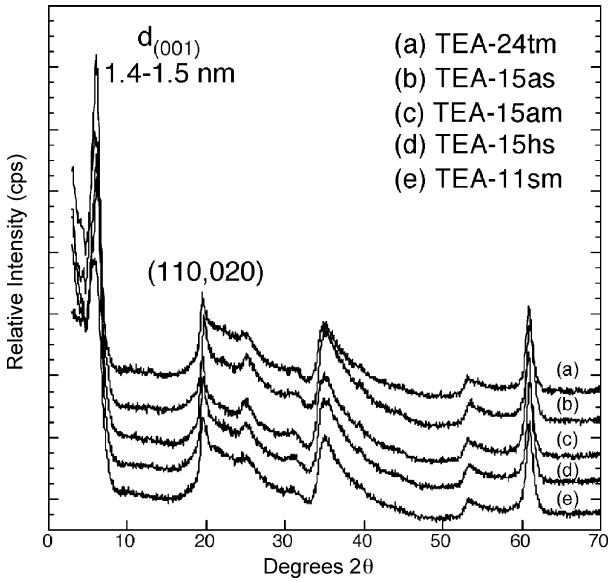


Fig. 1. XRD patterns of synthetic TEA–hectorite catalyst precursors.

## 3. Results and discussion

### 3.1. Synthetic clays

The XRD patterns shown in Fig. 1 are for as-prepared clay supports prior to calcination and metal loading. This figure contains the TEA-clays and the $d_{(0\,0\,1)}$-spacing is 1.4–1.5 nm. This value is lower, 1.2–1.3 nm, for the Li-clays due to the smaller size of this exchangeable cation. After calcination, the patterns look the same except that the *d*-spacing collapses to 1.0 nm. The XRD patterns were used as a qualitative measure of crystallinity of the support. Generally, the more intense and resolved the (0 0 1) basal reflection, the peak at 20° 2$\theta$ (the (1 1 0, 1 0 2) reflection) and the peak at 25° 2$\theta$ (the (0 0 4) reflection), the more crystalline the clay. Going by this measure, the most crystalline samples are derived from the 15 nm sols (AM30, AS30, and HS30). The same holds true for the Li-versions (figure not shown). The most intense basal spacing occurs for the AM30 sample.

The BET surface areas of samples after calcination ranged from 194 to 278 $m^2/g$ and pore volumes were generally 0.24–0.26 $cm^3/g$ for Li-clays and 0.41–0.49 $cm^3/g$ for those derived from TEA-clays. The isotherms were all Type IV with hysteresis loops. The vast majority of samples displayed H2 loops with the remainder having H3 loops. For those with H2 loops, which indicate mesostructuring, the average pore diameter size was typically 4.8–5.5 nm.

TEM of all of the clays prior to calcination was also performed. Two examples are shown in Fig. 2. Here, individual clay flakes and layers are visible as curved features approximately 100–200 nm long and some stacked layers on-edge can be observed. The background is dominated by spherical features, which are the unreacted silica particles. Although this latter phase appears to be dominant in TEM images due to contrast, it is in fact present at only about the 10 wt.% level [13a]. Also of importance to this study are the

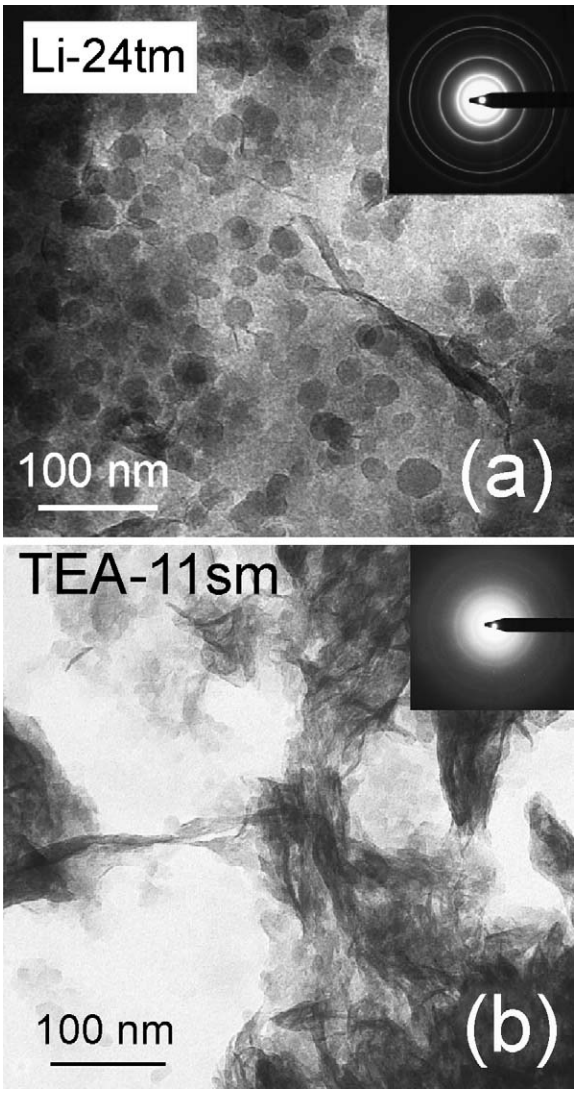


Fig. 2. TEM images with electron diffraction patterns of (a) Li-24tm and (b) TEA-11sm hectorites prior to calcination and catalyst loading.

differences apparent in the electron diffraction patterns. Note that Fig. 2a shows sharp, intense rings for Li-24tm indicating a high degree of crystallinity. Conversely, Fig. 2b shows only very weak and diffuse rings for TEA-11sm. These deductions were also apparent from the XRD patterns. Table 1 lists some of the clays used in terms of the precursor silica sol parameters. TEM was used to determine the particle size of the silica phase present in the clay as compared to the size in the sols provided by the supplier.

### 3.2. HDS of DBT

Table 2 summarizes HDS catalysis results in terms of %DBT conversion. The selectivity to biphenyl was 100% in all cases; no trace of the hydrogenation product cyclohexylbenzene was observed, nor was there any indication of hydrocracking. The reference, in contrast, which was a Crosfield 465 CoMoS–alumina catalyst, displayed a biphenyl yield of 80.8%, a cyclohexylbenzene yield of 5.0%, and a biphenyl selectivity of 94.2%. All catalysts maintained activity during the duration of the test. While %DBT conversions were considerably lower than that of the reference commercial catalyst, our interest was in parameters that may cause differences between the clays themselves. No correlation could be found for materials prior to CoMoS loading from $N_2$ porosimetry data. Interestingly, most of the catalysts displaying the highest DBT conversions were derived from the Li-clays (56.1–64.8%); TEA-15hs was also in this range at 58.3%. The remainder of the TEA-clays exhibited lower conversions of 40.1–49.6%. The activity results for the clays are especially encouraging considering the metal loadings. In particular, the mesostructured clays are loaded with 6 wt.% Mo and 2 wt.% Co which is in contrast to the nearly doubled loadings on the commercial Crosfield 465 catalyst as provided by the supplier (12.3 wt.% Mo, 3.8 wt.% Co) [16]. The loadings of Co and Mo were set by previous catalyst/support work in which the interest was improving the effectiveness of the metals. The objective of this work was not to supersede commercial catalyst performance per se. Rather, the interest lies in identifying more promising support alternatives, specifically synthetic clays, to advance hydrotreating catalyst development.

Table 2
HDS at 400 °C with CoMoS catalysts

| Catalyst support | %DBT conversion |
|---|---|
| Crosfield 465 | 85.8 |
| Li-15as | 64.8 |
| TEA-15hs | 58.3 |
| Li-24tm | 58.2 |
| Li-15hs | 56.1 |
| TEA-15as | 49.6 |
| TEA-24tm | 45.7 |
| TEA-15am | 44.3 |
| TEA-11sm | 40.1 |

The biphenyl selectivity was 100% in all cases except Crosfield 456 (CoMoS–alumina commercial catalyst), where it was 94.2%.

### 3.3. Deep HDS of 4,6-DMDBT

Tables 3 and 4 contain conversion and product selectivity data for this reaction over many of the same catalysts. The

Table 3
Deep HDS with CoMoS-clay catalysts

| Catalyst support | %DMDBT conversion at 325 °C | HYD/DDS at 325 °C[a] | %DMDBT conversion at 350 °C | HYD/DDS at 350 °C[a] |
|---|---|---|---|---|
| Criterion 344 | 11.4 | 2.2 | n.d. | n.d. |
| TEA-15am | 10.5 | 4.4 | 16.1 | 2.2 |
| TEA-15as | 9.5 | 3.6 | 14.2 | 1.9 |
| TEA-24tm | 5.9 | 2.8 | 10.4 | 1.9 |
| Li-24tm | 6.0 | 3.5 | 10.1 | 1.5 |
| TEA-15hs | 7.1 | 3.6 | 10.0 | 2.3 |
| TEA-11sm | 6.9 | 3.5 | 9.5 | 2.0 |
| Laponite | 3.0 | 2.3 | 2.9 | 1.5 |

Criterion 344 CoMoS–alumina commercial catalyst. n.d.: not determined.
[a] Ratio of hydrogenation products (HYD) over direct desulfurization products (DDS) (see Table 4).

Table 4
Product selectivity (%) from deep HDS at 325 °C

| Catalyst support | DMBP (DDS) | HDMDBT (HYD w/S) | MCHT (HYD w/o S) | HYD/DDS |
|---|---|---|---|---|
| TEA-15am | 18.7 | 58.4 | 22.9 | 4.4 |
| TEA-15as | 21.7 | 60.1 | 18.1 | 3.6 |
| TEA-15hs | 21.9 | 63.0 | 15.1 | 3.6 |
| TEA-11sm | 22.6 | 56.4 | 21.0 | 3.5 |
| Li-24tm | 22.4 | 52.7 | 24.9 | 3.5 |
| TEA-24tm | 26.6 | 53.3 | 20.1 | 2.8 |
| Laponite | 31.6 | 37.8 | 30.6 | 2.3 |
| Cr344 ($Al_2O_3$) | 31.0 | 19.1 | 49.9 | 2.2 |

DMBP: dimethyl biphenyl; HDMDBT: tetrahydrodimethyl dibenzothiophene; MCHT: methylcyclohexyltoluene. Cr344: Criterion 344 CoMoS–alumina commercial catalyst.

conversion of DMDBT was kept intentionally low for accurate kinetic studies. At 325 °C, the conversion of DMDBT over the Cr344 commercial catalyst was only 11.4% under these conditions. The reactivity of the most active catalyst, TEA-15am, was quite similar at 10.5%. As expected, the conversion increases with temperature; for example, the conversion is 16.1% for TEA-15am at 350 °C. The most active catalysts in this case are, generally, derived from the TEA-series and the 15 nm sols. Also note that laponite performs quite poorly at 3% conversion. This clay is also a synthetic hectorite and it is available commercially. However, compared to our synthetic clays, laponite is of smaller particle size and contains no mesostructuring due to the lack of incorporated silica.

There have been recent reports comparing the activity of catalysts in terms of hydrogenation (HYD) versus direct desulfurization (DDS) pathways that are operative during deep HDS [3,15,17]. After hydrogenation of DMDBT, elimination of the sulfur atom is facilitated due to molecular puckering. This puckering decreases the steric hindrance due to the methyl groups and increases the electron density of the sulfur atom [15,17]. It has become useful to compare the HYD/DDS ratio for this purpose. At 325 °C the HYD/DDS ratio for the commercial Cr344 catalyst is 2.2. Note that it is significantly higher, at 4.4, for the TEA-15am catalyst. The ratio is in fact higher for all of the clay catalysts. As shown in Table 3, increasing the temperature of HDS from 325 to 350 °C increased the conversion of 4,6-DMDBT with all clay-supported catalysts except laponite. In all of these cases, the HYD/DDS ratio decreased with increasing temperature, indicating that the hydrogenation (HYD) pathway is suppressed and the direct C–S bond hydrogenolysis (DDS) pathway is enhanced at higher temperature.

It is known that NiMoS-catalysts have higher activity for deep HDS than CoMoS-catalysts because the former usually has a higher hydrogenation activity [1]. In fact, a reference Cr424 NiMoS commercial catalyst showed 24.5% DMDBT conversion (and HYD/DDS ratio of 5.0) under the same conditions at 325 °C where the Cr344 CoMoS catalyst showed 11.4% conversion (HYD/DDS = 4.4). Since all of the clay supports show higher HYD activity than Cr344, it would be expected that use of NiMoS would increase activity even further. The TEA-15am support, moreover, displays activities (%DMDBT conversions) that are very similar to the HDS activity of the commercial CoMoS-catalyst. If this material were to be modified further by different preparation methods or pretreatments, it shows potential as a promising deep HDS catalyst. Future studies will focus on testing these supports as NiMoS-catalysts.

Table 5
$N_2$ porosimetry of various DBT HDS catalysts

| Stage | Surface area ($m^2/g$) | Pore volume ($cm^3/g$) | Hysteresis loop type |
|---|---|---|---|
| TEA-15hs | | | |
| Calcined | 225 | 0.38 | H2 |
| After CoMoS | 143 | 0.27 | H2 |
| After HDS | 99 | 0.22 | H2 |
| Li-15as | | | |
| Calcined | 200 | 0.24 | H2 |
| After CoMoS | 125 | 0.15 | H2 |
| After HDS | 65 | 0.10 | H2 |
| TEA-11sm | | | |
| Calcined | 278 | 0.46 | H2 |
| After CoMoS | 115 | 0.25 | H3 |
| After HDS | 78 | 0.22 | H3 |

### 3.4. Catalyst stability

XRD, $N_2$ porosimetry, and TEM characterization of some of the materials was done after CoMoS loading and after DBT HDS catalysis. For these purposes, only the most reactive (TEA-15hs, Li-15as) and least reactive (TEA-11sm) catalysts were examined. Table 5 provides the $N_2$ porosimetry data for these particular samples. As would be expected, the surface areas and pore volumes decrease quite markedly upon CoMoS loading of the supports, and further still after HDS reaction. The one parameter that changes for the least active catalyst (TEA-11sm) that does not change for the active catalysts is the hysteresis loop type. In Fig. 3, it is apparent that this loop changes from H2 to H3 upon CoMoS loading. This indicates that the mesostructuring of this material is lost upon metal loading, and may be related to the low degree of crystallinity of this support (from XRD and TEM data). The isotherms of all the TEA-clay supports are very similar to that of Fig. 3a. Isotherms for the Li-clay supports differ slightly, especially in the desorption branch, but they are all similar to each other. An example for calcined Li-15hs is shown in Fig. 3c.

The high resolution TEM image shown in Fig. 4 is for the CoMoS–Li-15as active catalyst. Note the curved, multi-layered structure that nearly envelops one of the silica particles and the lattice fringes in the upper left portion of the image. Both are assumed to arise from the CoMoS-species since neither has been observed in the precursor clay supports. In a similar system, Li et al. [18] examined a series of mixed $ZrO_2$–$Al_2O_3$ supports with different amorphous $ZrO_2$ contents, all confirmed at about 5 nm in size and well dispersed in the alumina. Sulfided CoMo catalysts supported on these mixed supports showed a higher

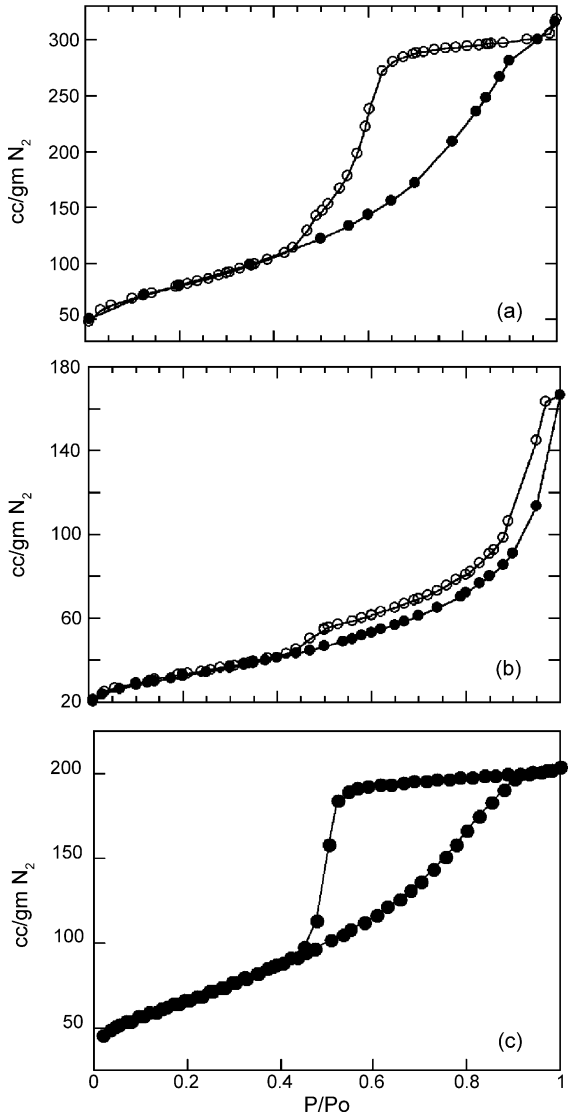


Fig. 3. $N_2$ isotherms for calcined TEA-11sm (a) before and (b) after CoMoS-loading; solid circles = adsorption, open circles = desorption; (c) calcined Li-15hs.

DBT HDS activity than those supported on alumina and a commercial HDS catalyst. Further, it was found by HR-TEM that the $ZrO_2$ had a clear effect on the sulfide component's morphology; a multilayered structure of CoMoS was formed on the $ZrO_2$–$Al_2O_3$ supports while a mono-layered structure was formed on $Al_2O_3$. It was assumed that the multilayered CoMoS on the mixed supports provided more active sites, and that assumption is reinforced by the present results. Reports of $MoS_2$-based layers on sulfided CoMoS catalysts using support materials such as Al-MCM-41 also have been reported recently [19]. The stacking degree of $MoS_2$-based layers on the synthetic clays appears to be higher than was indicated for this mesoporous silica. The presence of a multilayered MoS morphology, therefore, has been demonstrated as important in the literature. We conclude that the unique morphology of the synthetic clay supports lends them amenable to formation of this more active phase.

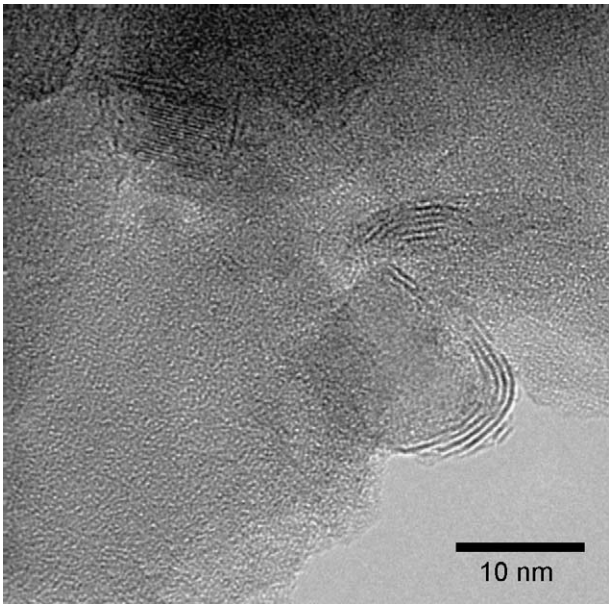


Fig. 4. HR-TEM image of CoMoS–Li-AS30.

## 4. Conclusions

The work described here comprises an exploratory study to examine mesostructured synthetic clays as supports for hydrotreating catalysts. It is significant that different nanoporous silica supports with similar chemical composition (e.g. mesoporous silica versus silicalite) but different pore structure have been shown to lead to significantly different activity and selectivity features for deep HDS of 4,6-DMDBT. Synthetic clays offer another, unique, porous structure of similar, silica-based composition. Among the clay supports, precursor silica sols that yield silica particle sizes of 15 nm appear to be optimum for both HDS and deep HDS reactions. Both smaller and larger silica sol sizes were employed, but both showed a negative effect on final catalytic results. The 15 nm sols foster the most crystalline materials (from XRD and TEM data) and the optimum mesostructuring (in terms of textural porosity and morphology) of the clay catalyst precursor. This may also have an impact on the optimum CoMoS-species size and/or shape, which warrants more extensive HR-TEM imaging of metal loaded catalysts in the future.

Variation between the activity of a particular catalyst for HDS versus deep HDS is not directly comparable due to differences in conditions such as calcination, CoMoS-loading, and reaction temperatures. It is notable, however, that the synthetic clays display extremely low hydrogenation in HDS. Since hydrogenation decreases with increasing temperature for deep HDS, a comparison at 400 °C would be warranted in this regard. The Li-clays are overall more active for DBT HDS than the TEA-versions, while the reverse is true for deep DMDBT HDS. The Li-clays appear from XRD and TEM/ED to be more crystalline than the TEA versions. Since the HDS was carried out at 400 °C and the deep HDS carried out at just 325–350 °C, the higher degree of crystallinity may be manifesting itself in reaction temperature stability. Another factor to consider is that

the Li-versions have lower pore volumes at 0.24–0.26 $cm^3/g$ than the TEA-clay supports at 0.41–0.49 $cm^3/g$. Deep HDS studies with the mesostructured clays that are loaded with NiMoS are in progress and will be reported in the future.

## Acknowledgements

R. Fernandez-Saavedra of the Institute of Materials Science, Consejo Superior de Investigaciones Cientificas (CSIC), Madrid, Spain, under a fellowship from the CICYT, is acknowledged. R.E. Cook of MSD-ANL acquired TEM images of pure clay samples at the ANL Electron Microscopy Center. The TEM facility at the Cummings Life Science Center of the University of Chicago is acknowledged. This work was performed under the auspices of the U.S. DOE, Office of Basic Energy Sciences, Division of Chemical Sciences, Geosciences, and Biosciences under contract no. W-31-109-ENG-38.

## References

[1] (a) S.K. Bej, S.K. Maity, U.T. Turaga, Energy Fuels 18 (2004) 1227;
(b) C.S. Song, Catal. Today 86 (2003) 211.
[2] (a) J. Cinibulk, P.J. Kooyman, Z. Vit, M. Zdrazil, Catal. Lett. 89 (2003) 147;
(b) A.M. Venezia, V. La Parola, G. Deganello, D. Cauzzi, G. Leonardi, G. Predieri, Appl. Catal. A 229 (2002) 261;
(c) S.K. Maity, M.S. Rana, S.K. Bej, J. Ancheyta-Juarez, G. Murali Dhar, T.S.R.P. Rao, Appl. Catal. A: Gen. 205 (2001) 215;
(d) S.K. Maity, M.S. Rana, B.N. Srinivas, S.K. Bej, G. Murali Dhar, T.S.R.P. Rao, J. Mol. Catal. A: Chem. 153 (2000) 121;
(e) S.K. Maity, M.S. Rana, S.K. Bej, J. Ancheyta-Juarez, G. Murali Dhar, T.S.R.P. Rao, Catal. Lett. 72 (2001) 115;
(f) D. Wang, W. Qian, A. Ishihara, T. Kabe, J. Catal. 290 (2002) 266;
(g) S. Dzwigaj, C. Louis, M. Breysee, M. Cattenot, V. Bellie're, C. Geantet, M. Vrinat, P. Blanchard, E. Payen, S. Inoue, H. Kudo, Y. Yoshimura, Appl. Catal. B 41 (2003) 181;
(h) S. Damyanova, S. Andonova, I. Stereva, C. Vladov, L. Petrov, P. Grange, React. Kinet. Catal. Lett. 79 (2003) 35.
[3] M.V. Landau, D. Berger, J. Herskowitz, J. Catal. 159 (1996) 236.
[4] (a) U.T. Turaga, X. Ma, C.S. Song, Catal. Today 86 (2003) 265;
(b) U.T. Turaga, C.S. Song, Catal. Today 86 (2003) 129;
(c) M. Breysse, P. Afanasiev, C. Geantet, M. Vrinat, Catal. Today 86 (2003) 5;
(d) C.S. Song, X. Ma, Int. J. Green Energy 41 (2004) 167;
(e) T. Isoda, Y. Takase, K. Kusakabe, S. Morooka, Energy Fuels 14 (2000) 585.
[5] F. Bataille, J.L. Lemberton, G. Perot, P. Leyrit, T. Cseri, N. Marchal, S. Kasztelan, Appl. Catal. A 220 (2001) 191.
[6] (a) C.S. Song, K.M. Reddy, Appl. Catal. A 176 (1999) 1;
(b) A. Wang, Y. Wang, T. Kabe, Y. Chen, A. Yshihara, W. Quian, J. Catal. 199 (2001) 19;
(c) A. Wang, Y. Wang, T. Kabe, Y. Chen, A. Yshihara, W. Qian, P. Yao, J. Catal. 210 (2002) 319;
(d) T. Klimova, M. Calderon, J. Ramirez, Appl. Catal. A 240 (2003) 29.
[7] C. Song, X. Ma, Appl. Catal. B: Environ. 41 (2003) 207.
[8] S.M. Auerbach, K.A. Carrado, P.K. Dutta (Eds.), Handbook of Layered Materials, Marcel-Dekker, New York, 2004.
[9] (a) J.A. Colin, J.A. de los Reyes, A. Vazquez, A. Montoya, Appl. Surf. Sci. 240 (2005) 48;
(b) P. Salerno, S. Mendioroz, A.L. Agudo, Appl. Catal. A: Gen. 259 (2004) 17;
(c) P. Salerno, S. Mendioroz, A.L. Agudo, Appl. Clay Sci. 23 (2003) 287;
(d) M. Sychev, R. Prihod'ko, A. Koryabkina, E.J. Hensen, J.A.R. van Veen, R.A. van Santen, Scientific basis for the preparation of heterogeneous catalysts, Stud. Surf. Sci. Catal. 143 (2002) 257;
(e) P. Salerno, M.B. Asenjo, S. Mendioroz, Thermochim. Acta 379 (2001) 111;
(f) S.A. Ali, M.E. Biswas, T. Yoneda, T. Miura, H. Hamid, E. Iwamatsu, H. Al-Suaibi, Science and technology in catalysis, Stud. Surf. Sci. Catal. 121 (1998) 407;
(g) C.E. Ramos-Galvan, G. Sandoval-Robles, A. Castillo-Mares, J.M. Dominguez, Appl. Catal. A: Gen. 150 (1997) 37.
[10] M.M. Hossain, M.A. Al-Saleh, M.A. Shalabi, T. Kimura, T. Inui, Appl. Catal. A: Gen. 278 (2004) 65.
[11] (a) K.A. Carrado, Appl. Clay Sci. 17 (2000) 1;
(b) K. Carrado Gregar, R.E. Winans, R.E. Botto, US Patent 5,308,808 (1994).
[12] K.A. Carrado, R. Csencsits, P. Thiyagarajan, S. Seifert, S.M. Macha, J.S. Harwood, J. Mater. Chem. 12 (2002) 3228.
[13] (a) K.A. Carrado, L. Xu, Micropor. Mesopor. Mater. 27 (1999) 87;
(b) K.A. Carrado, L. Xu, C.L. Marshall, D. Wei, S. Seifert, C.A. Bloomquist, in: A. Sayari, M. Jaroniec, T.J. Pinnavaia (Eds.), Nanoporous Materials II: Stud. Surf. Sci. Catal., vol. 129, Elsevier, Amsterdam, 2000, p. 417.
[14] R.E. Grim, Clay Mineralogy, McGraw-Hill, New York, 1968, p. 68.
[15] J.H. Kim, X. Ma, C.S. Song, Y.K. Lee, S.T. Oyama, Energy Fuels 19 (2005) 353.
[16] G.R. Wilson, N.L. Carr, US Patent 5,780,381 (1998).
[17] (a) X. Ma, K. Sakanishi, T. Isoda, I. Mochida, Energy Fuels 9 (1995) 33.
[18] G.R. Li, W. Li, M.H. Zhang, K.Y. Tao, Appl. Catal. A: Gen. 273 (2004) 233.
[19] P.J. Kooyman, P. Waller, A.D. van Langeveld, C.S. Song, K.M. Reddy, J.A.R. van Veen, Catal. Lett. 90 (2003) 131.